

(19)



(11)

**EP 1 673 013 B1**

(12)

**EUROPEAN PATENT SPECIFICATION**

(45) Date of publication and mention  
of the grant of the patent:  
**20.10.2010 Bulletin 2010/42**

(51) Int Cl.:  
**A61B 8/08** (2006.01) **G01S 15/89** (2006.01)  
**G06F 19/00** (2006.01)

(21) Application number: **04744758.6**

(86) International application number:  
**PCT/IB2004/051416**

(22) Date of filing: **06.08.2004**

(87) International publication number:  
**WO 2005/030057 (07.04.2005 Gazette 2005/14)**

**(54) ULTRASONIC CARDIAC VOLUME QUANTIFICATION**

ULTRASCHALLQUANTIFIZIERUNG DES HERZVOLUMENS

QUANTIFICATION ULTRASONORE DU VOLUME CARDIAQUE

(84) Designated Contracting States:  
**AT BE BG CH CY CZ DE DK EE ES FI FR GB GR  
HU IE IT LI LU MC NL PL PT RO SE SI SK TR**

(30) Priority: **29.09.2003 US 507263 P**

(43) Date of publication of application:  
**28.06.2006 Bulletin 2006/26**

(73) Proprietor: **Koninklijke Philips Electronics N.V.  
5621 BA Eindhoven (NL)**

(72) Inventor: **SALGO, Ivan  
Bothell, WA 98041-3003 (US)**

(74) Representative: **Roche, Denis et al  
Philips IP&S France  
Société Civile SPID  
33 rue de Verdun  
BP 313  
92156 Suresnes Cedex (FR)**

(56) References cited:  
**US-A- 5 107 838 US-A- 5 465 721  
US-A1- 2002 072 671 US-A1- 2003 055 308**

**EP 1 673 013 B1**

Note: Within nine months of the publication of the mention of the grant of the European patent in the European Patent Bulletin, any person may give notice to the European Patent Office of opposition to that patent, in accordance with the Implementing Regulations. Notice of opposition shall not be deemed to have been filed until the opposition fee has been paid. (Art. 99(1) European Patent Convention).

## Description

**[0001]** This invention relates to ultrasonic diagnostic imaging and, more particularly, to ultrasonic imaging systems capable of estimating the volume of vessels and organs such as the heart.

**[0002]** Echocardiographic ultrasonic imaging systems are used to assess the performance of the heart. Cardiac performance can be assessed qualitatively with these systems, such as by observing the blood flow through vessels and valves and the operation of heart valves. Quantitative measures of cardiac performance can also be obtained with such systems. For instance, the velocity of blood flow and the sizes of organs and cavities such as a heart chamber can be measured. These measures can produce quantified values of cardiac performance such as ejection fraction and cardiac output. A method and apparatus for measuring the volume of a heart chamber are described in US patent 5,322,067 (Prater et al.), for example. In the method described in this patent, the clinician acquires a sequence of ultrasound images of a cavity to be measured, such as the left ventricle of the heart. The clinician freezes one of the images on the display screen and traces a fixed region of interest (ROI) around the cavity of the heart chamber. The defined ROI should be large enough to encompass the heart chamber when the heart is fully expanded. The ultrasound system then processes the pixels in the ROI in each image in the sequence to determine those pixel that are blood pixels in the left ventricle. Each left ventricle is then segmented into strips and the area of the strips is calculated. Each strip is then conceptually rotated about its center to define a disk and the volume of each disk is calculated. By summing the volumes of the disks in each image the volume of the heart chamber is determined at each point in the heart cycle for which an image was acquired. The calculated volumes can be displayed numerically as a function of time, or a waveform representative of left ventricle volume as a function of time can be produced, thereby showing the clinician the changes in left ventricular volume over the heart cycle.

**[0003]** The method of the Prater et al. patent requires manual input from the clinician who must define the ROI by a manual tracing. The method can only be performed on a stored image loop due to this need for manual input. It would be desirable for such a technique to be performed by the ultrasound system automatically and to be performed in true real time as the images are acquired. Furthermore, the method of disks (Simpson's rule) volume estimation assumes that each disk is uniformly circular, which may not be the case. It would be desirable to estimate cavity volumes that are more closely related to the true shape of the anatomy rather than having to rely on an assumption of geometric uniformity of the anatomy, thus producing more accurate volume measures.

**[0004]** US patent application publication 2002/0072671 describes a method for automatically tracing a tissue border in an ultrasonic image which compris-

es acquiring one or more images, locating anatomical landmarks in the image, fitting a border trace to the anatomical landmarks, and displaying an ultrasonic image in which a tissue border has been automatically traced.

Adjustable control points are located on the displayed border, enabling the automatically drawn border to be manually adjusted by a rubberbanding technique.

**[0005]** The invention is set out in claim 1. In accordance with the principles of the present invention, the volume of a body cavity or organ is measured by ultrasonic imaging. Cross-sectional images in different planes of the body cavity are acquired at substantially the same time, thus presenting views of the shape of the cavity at a point in time from different perspectives. A surface of the cavity or organ in each image is outlined by automated or semi-automated border tracing. Segments of the cavity are defined by producing a geometric model of the cavity or organ from the tracings. The segment volumes are accumulated to produce an accurate measure of the volume of the cavity. The inventive method can be performed in real time and produces a more accurate estimate of the cavity volume. The resulting measure can be displayed numerically or as a physiologic curve of the changing volume with time.

**[0006]** In the drawings:

FIGURE 1 is a four chamber ultrasound image of the heart.

FIGURE 2 illustrates an ultrasound display of both end diastole and end systole cardiac images.

FIGURES 3a and 3b illustrate the step of locating the medial mitral annulus (MMA) and the lateral mitral annulus (LMA) in an ultrasound image of the left ventricle (LV).

FIGURE 4 illustrates the step of locating the apex of the LV.

FIGURES 5a-5c illustrate standard border shapes for the LV.

FIGURES 6a-6b illustrate geometric templates used to locate the MMA and LMA.

FIGURES 7a-7c illustrate a technique for fitting a standard border shape to the endocardial boundary of the LV.

FIGURE 8 illustrates an end diastole and end systole display with endocardial borders drawn automatically in accordance with the principles of the present invention.

FIGURE 9 illustrates the rubber-banding technique for adjusting an automatically drawn border.

FIGURE 10 is a photograph of an actual ultrasound system display when operating in the biplane mode in accordance with the principles of the present invention.

FIGURE 11 illustrates in block diagram form an embodiment of an ultrasonic diagnostic imaging system constructed in accordance with the principles of the present invention.

FIGURE 12 illustrates an ultrasound display screen

produced in accordance with the principles of the present invention.

FIGURES 13a and 13b illustrate the formation of cavity segments from orthogonal views of the left ventricle.

**[0007]** Referring first to FIGURE 1, an ultrasound system display is shown during the acquisition of cardiac images. The ultrasound image 10 is a four-chamber view of the heart which is acquired by a phased array transducer probe to produce the illustrated sector-shaped image. The image shown is one of a sequence of real-time images acquired by placement of the probe for an apical 4-chamber view of the heart, in which the probe is oriented to view the heart from the proximity of its apex 11. The largest chamber in the image, in the central and upper right portion of the image, is the left ventricle (LV). As the real-time ultrasound image sequence is acquired a scrolling ECG trace 12 of the heart cycle is simultaneously acquired and displayed at the bottom of the display, with a triangular marker 14 denoting the point or phase of the cardiac cycle at which the currently-displayed image was acquired. A typical duration of the heart cycle when the body is at rest is about one second, during which time approximately 30-90 image frames of the heart can be acquired and displayed in rapid succession. As the clinician views the display of FIGURE 1, the heart is seen beating in real time in the ultrasound display as the ECG waveform 12 scrolls beneath the ultrasound images 10, with the instantaneously displayed heart phase indicated by the marker 14.

**[0008]** In one mode of acquisition, the clinician observes the beating heart in real time while manipulating the transducer probe so that the LV is being viewed distinctly in maximal cross-section. When the four chamber view is being acquired continuously and clearly, the clinician depresses the "freeze" button to retain the images of the current heart cycle in the image frame or Cineloop® memory of the ultrasound system. The Cineloop memory will retain all of the images in the memory at the time the freeze button is depressed which, depending upon the size of the memory, may include the loop being viewed at the time the button was depressed as well as images of a previous or subsequent loop. A typical Cineloop memory may hold 400 image frames, or images from about eight to ten heart cycles. The clinician can then scan through the stored images with a trackball, arrow key, or similar control to select the loop with the images best suited for analysis. When the clinician settles on a particular loop, the "ABD" protocol is actuated to start the border drawing process.

**[0009]** When the ABD protocol is actuated the display changes to a dual display of the end diastole image 16 and the end systole image 18 displayed side-by-side as shown in FIGURE 2. The ultrasound system identifies all of the images comprising the selected loop by the duration of the ECG waveform associated with the selected loop. The ultrasound system also recognizes the end di-

astole and end systole points of the cardiac cycle in relation to the R-wave of the ECG waveform 12 and thus uses the ECG waveform R-wave to identify and display the ultrasound images at these two phases of the heart cycle. The dual display of FIGURE 2 shows the ECG waveform 12 for the selected heart cycle beneath each ultrasound image, with the marker 14 indicating the end diastole and end systole phases at which the two displayed images were acquired.

**[0010]** Since the Cineloop memory retains all of the images of the cardiac cycle, the user has the option to review all of the images in the loop, including those preceding and succeeding those shown in the dual display. For instance, the clinician can "click" on either of the images to select it, then can manipulate the trackball or other control to sequentially review the images which precede or succeed the one selected by the ultrasound system. Thus, the clinician can select an earlier or later end diastole or end systole image from those selected by the ultrasound system. When the clinician is satisfied with the displayed images 16 and 18, the ABD processor is actuated to automatically delineate the LV borders on the two displayed images as well as the intervening undisplayed images between end diastole and end systole.

**[0011]** In this example the ABD processor begins by drawing the endocardial border of the LV in the end systole image 18. The first step in drawing the border of the LV is to locate three key landmarks in the image, the medial mitral annulus (MMA), the lateral mitral annulus (LMA), and the endocardial apex. This process begins by defining a search area for the MMA as shown in FIGURE 3a, in which the ultrasound image grayscale is reversed from white to black for ease of illustration. Since the ABD processor is preconditioned in this example to analyze four-chamber views of the heart with the transducer 20 viewing the heart from its apex, the processor expects the brightest vertical nearfield structure in the center of the image to be the septum which separates the left and right ventricles. This means that the column of pixels in the image with the greatest total brightness value should define the septum. With these cues the ABD processor locates the septum 22, and then defines an area in which the MMA should be identified. This area is defined from empirical knowledge of the approximate depth of the mitral valve from the transducer in an apical view of the heart. A search area such as that enclosed by the box 24 in FIGURE 3a is defined in this manner.

**[0012]** In this embodiment a filter template defining the anticipated shape of the MMA is then cross correlated to the pixels in the MMA search area. While this template may be created from expert knowledge of the appearance of the MMA in other four-chamber images as used by Wilson et al. in their paper "Automated analysis of echocardiographic apical 4-chamber images," Proc. of SPIE, August, 2000, a geometric corner template may be used as follows. While a right-angle corner template may be employed, in a constructed embodiment an octagon corner template 28 (the lower left corner of an oc-

tagon) is used as the search template for the MMA, as shown at the right side of FIGURE 6a. In practice, the octagon template is represented by the binary matrix shown at the left side of FIGURE 6a. The ABD processor performs template matching by cross correlating different sizes of this template with the pixel data in different translations and rotations until a maximum correlation coefficient above a predetermined threshold is found. To speed up the correlation process, the template matching may initially be performed on a reduced resolution form of the image, which highlights major structures and may be produced by decimating the original image resolution. When an initial match of the template is found, the resolution may be progressively restored to its original quality and the location of the MMA progressively refined by template matching at each resolution level.

**[0013]** Once the MMA has been located a similar search is made for the location of the LMA, as shown in FIGURE 3b. The small box 26 marks the location established for the MMA in the image 18, and a search area to the right of the MMA is defined as indicated by the box 34. A right corner geometric template, preferably a right octagon corner template 38 as shown in FIGURE 6b, is matched by cross-correlation to the pixel values in the search area of box 34. Again, the image resolution may be decimated to speed the computational process and different template sizes may be used. The maximal correlation coefficient exceeding a predetermined threshold defines the location of the LMA.

**[0014]** With the MMA 26 and the LMA 36 found, the next step in the process is to determine the position of the endocardial apex, which may be determined as shown in FIGURE 4. The pixel values of the upper half of the septum 22 are analyzed to identify the nominal angle of the upper half of the septum, as indicated by the broken line 43. The pixel values of the lateral wall 42 of the LV are analyzed to identify the nominal angle of the upper half of the lateral wall 42, as shown by the broken line 45. If the lateral wall angle cannot be found with confidence, the angle of the scanlines on the right side of the sector is used. The angle between the broken lines 43,45 is bisected by a line 48, and the apex is initially assumed to be located at some point on this line. With the horizontal coordinate of the apex defined by line 48, a search is made of the slope of pixel intensity changes along the line 48 to determine the vertical coordinate of the apex. This search is made over a portion of line 48 which is at least a minimum depth and not greater than a maximum depth from the transducer probe, approximately the upper one-quarter of the length of line 48 above the mitral valve plane between the MMA 26 and the LMA 36. Lines of pixels along the line 48 and parallel thereto are examined to find the maximum positive brightness gradient from the LV chamber (where there are substantially no specular reflectors) to the heart wall (where many reflectors are located). A preferred technique for finding this gradient is illustrated in FIGURE 7. FIGURE 7a shows a portion of an ultrasound image including a

section of the heart wall 50 represented by the brighter pixels in the image. Drawn normal to the heart wall 50 is a line 48 which, from right to left, extends from the chamber of the LV into and through the heart wall 50. If the pixel values along line 48 are plotted graphically, they would appear as shown by curve 52 in FIGURE 7b, in which brighter pixels have greater pixel values. The location of the endocardium is not the peak of the curve 52, which is in the vicinity of the center of the heart wall, but relates to the sense of the slope of the curve. The slope of the curve 52 is therefore analyzed by computing the differential of the curve 52 as shown by the curve 58 in FIGURE 7c. This differential curve has a peak 56 which is the maximal negative slope at the outside of the heart wall (the epicardium). The peak 54, which is the first major peak encountered when proceeding from right to left along curve 58, is the maximal positive slope which is the approximate location of the endocardium. The pixels along and parallel to line 48 in FIGURE 4 are analyzed in this manner to find the endocardial wall and hence the location of the endocardial apex, marked by the small box 46 in FIGURE 4.

**[0015]** If the user is operating on a sequence of stored images, the three points could be defined manually. For example, the user could point at the three landmarks in an image of the sequence with a pointing device such as a mouse or trackball, then click on them as they are identified to mark them in the image.

**[0016]** Once these three major landmarks of the LV have been located, one of a number of predetermined standard shapes for the LV is fitted to the three landmarks and the endocardial wall. Three such standard shapes are shown in FIGURES 5a, 5b, and 5c. The first shape, border 62, is seen to be relatively tall and curved to the left. The second shape, border 64, is seen to be relatively short and rounded. The third shape, border 66, is more triangular. Each of these standard shapes is scaled appropriately to fit the three landmarks 26,36,46. After an appropriately scaled standard shape is fit to the three landmarks, an analysis is made of the degree to which the shape fits the border in the echo data. This may be done, for example, by measuring the distances between the shape and the heart wall at points along the shape. Such measurements are made along paths orthogonal to the shape and extending from points along the shape. The heart wall may be detected using the operation discussed in FIGURES 7a-7c, for instance. The shape which is assessed as having the closest fit to the border to be traced, by an average of the distance measurements, for instance, is chosen as the shape used in the continuation of the protocol.

**[0017]** The chosen shape is then fitted to the border to be traced by "stretching" the shape, in this example, to the endocardial wall. The stretching is done by analyzing 48 lines of pixels evenly spaced around the border and approximately normal to heart wall. The pixels along each of the 48 lines are analyzed as shown in FIGURES 7a-7c to find the adjacent endocardial wall and the cho-

sen shape is stretched to fit the endocardial wall. The baseline between points 26 and 36 is not fit to the shape but is left as a straight line, as this is the nominal plane of the mitral valve. When the shape has been fit to points along the heart wall, the border tracing is smoothed and displayed over the end systole image as shown in the image 78 on the right side of the dual display of FIGURE 8. The display includes five control points shown as X's along the border between the MMA landmark and the apex, and five control points also shown as X's along the border between the apex landmark and the LMA landmark. In this example the portion of line 48 between the apex and the mitral valve plane is also shown, as adjusted by the stretching operation.

**[0018]** Since each of the images shown in FIGURE 8 is one image in a cardiac loop of images, the clinician can further verify the accuracy of the borders of the end diastole and end systole images 76,78 by playing a saved cardiac loop of images behind the borders drawn on the display of FIGURE 8. This is done by selecting one of the images of FIGURE 8, then selecting "Play" from the system menu to repetitively play the saved cardiac loop in real time or at a selected frame rate of display behind the border. In the end diastole image 76 the endocardium is at its maximum expansion; hence, the endocardium in the loop should appear to move inward from and then back to the endocardial border drawn on the end diastole image. In the end systole image 78 the endocardium is fully contracted; hence, the endocardium in the loop should appear to move outward and then back to the border in this image. If the endocardium does not move in this manner and, for example, is seen to pass through the border, a different image may need to be chosen for end diastole or end systole, or manual adjustment of a drawn border may be necessary. Of course, the loop and its drawn borders over the complete cardiac cycle can be replayed, enabling the clinician to view to endocardial tracing as it changes with the heart motion in real time.

**[0019]** Images with automatically traced borders which are saved in memory can be recalled and their automatically drawn borders refined by manual adjustment, if desired. This process is known as "rubberbanding." As FIGURE 8 shows, the endocardial borders of both the end diastole and end systole images have small boxes denoting the three major landmarks and control points marked by X's on the septal and lateral borders. The clinician chooses the default number of control point which will be displayed initially; on the border 80 shown in FIGURE 9 there are three control points shown on the septal wall and four control points shown on the lateral wall. The clinician can review the end diastole and systole images, as well as all of the intervening images of the stored loop if desired, and manually adjust the positions of the landmark boxes and control point X's if it is seen that the automated process placed a border in an incorrect position. The clinician can slide a box or X along the border to a new position, and can add more control points or delete control points from the border. Suppose that

the ABD processor had initially located the control point and border at the position shown by circle 82 and dashed line 84, which the clinician observes is incorrect. The clinician can relocate the control point laterally by dragging the X with a screen pointing device to the new location as shown by 86. As the X is dragged, the border moves or stretches along with the X, thereby defining a new border as shown by the solid line border 88. In this manner the clinician can manually correct and adjust the borders drawn by the ABD processor.

**[0020]** As the ABD processor is identifying the key landmarks and fitting borders to the sequence of images, it is periodically making confidence measurements to gauge the likelihood that the image borders are being accurately located and traced. For instance, if the septum is not clearly contrasted from the blood pool in the LV chamber, the automated process will stop. If the various correlation coefficients do not exceed predetermined thresholds the process will stop. Both spatial and temporal confidence measurements are employed. For instance, if the computed border of an image varies too much from a standard shape in either size or shape, the process will abort. This can arise if the landmarks are located in unusual positions in relation to each other, for example. If the change in the computed border from one image in the sequence to another is too great, the process will likewise abort. When the process stops, a message is displayed notifying the clinician of the reason for stopping the process, and gives the clinician the option to continue the automated process, to continue the automated process with or after clinician input, or for the clinician to acquire a new loop of images or manually trace the current images.

**[0021]** In the illustrated example of FIGURE 8 the automatically drawn borders of the end diastole and end systole images are used to compute the heart's ejection fraction. This is done by an automatic modified Simpson's rule process which divides the delineated heart chamber at each phase into a stack of virtual disks. The diameter of each disk is used with the disk height to compute an effective volume of each disk, and these volumes are summed to compute the heart chamber volume at both end diastole and end systole. The difference between the two yields the ejection fraction, the volume or percentage of the heart volume which is expelled as pumped blood during each heart cycle. The ejection fraction calculation is shown in the measurement box at the lower left hand corner of FIGURE 8 and is constantly updated. Thus, if the clinician should adjust a drawn border by the rubberbanding technique, the computed volume of the heart during that phase will change, affecting the ejection fraction calculation, and the new calculation immediately appears in the measurement box. As the clinician adjusts the drawn borders he instantaneously sees the effects of these changes on the calculation of the ejection fraction.

**[0022]** FIGURE 10 illustrates biplane images which may be used in an embodiment of the present invention.

As used herein the term "biplane images" refers to two images which are simultaneously acquired from different planes of a volumetric region of the body. Two images are acquired simultaneously when they are acquired in the same short time interval, which may be accomplished by acquiring the first and second images in rapid succession or by interleaved acquisition of scanlines from the two image planes until the two images have been fully acquired. US patent 6709394 entitled "BIPLANE ULTRASONIC IMAGING", and of which I am a co-inventor describes two biplane modes. In the biplane implementation described in this patent, one image is acquired in a plane normal to the center of a two dimensional array transducer and the other image is initially in a plane centered with the first image but in a plane orthogonal to that of the first image. One of the images may then be relocated by either the "tilt" mode of operation or the "rotate" mode of operation. In the tilt mode, the second image is inclined to another image plane which intersects another scanline of the first image while remaining in an orthogonal orientation with the first image. The second image may be tilted from alignment with the center of the first image to alignment with the lateral scanlines of the first image or in alignment with any scanline between these extremes. In the rotate mode the two images retain their common centerline alignment but the second image plane is rotated about this centerline. The second image can be rotated from its initial orthogonal relationship with the first image to the same image plane as the first image, or at any rotation therebetween. FIGURE 10 shows two biplane images in the rotate mode. The left image is a four-chamber heart image like those shown previously and the right image is orthogonal to the first and shows the left ventricle as it appears when intersected by the plane of the second image. The circular white icon between the two images in the center of the screen shows that the right image plane has been rotated ninety degrees from alignment with the left reference image plane. Marker dots are clearly visible in the icon and on the right sides of the apexes of the two sector images, indicating the left-right orientation of the two images. For completeness of a cardiac study the EKG trace is also shown below the biplane images.

**[0023]** An advantage of the present invention is that since only two planes of a volumetric region are being imaged, acquisition of the two images can be done rapidly enough so that the two images can both be real-time ultrasonic images at a relatively high frame rate of display. Moreover, the two images are of the heart at substantially the same point in time and are thus concurrently acquired images for purposes of the invention. A further advantage is that the ultrasound system need be only a conventional two dimensional imaging system. As FIGURE 11 will illustrate, the display subsystem for biplane imaging can be a conventional two dimensional image processing subsystem, which means that biplane imaging in accordance with the present invention can be done with the two dimensional ultrasound systems currently in

the hands of clinicians. The scanner and display subsystem of FIGURE 11 needs no unique 3D capabilities in order to produce the biplane image shown in FIGURE 10.

**[0024]** Referring now to FIGURE 11, an ultrasound system constructed in accordance with the principles of the present invention is shown in block diagram form. In this embodiment an ultrasound probe 110 includes a two dimensional array transducer 500 and a micro-beamformer 502. The micro-beamformer contains circuitry which controls the signals applied to groups of elements ("patches") of the array transducer 500 and does some processing of the echo signals received by elements of each group. Micro-beamforming in the probe advantageously reduces the number of conductors in the cable 503 between the probe and the ultrasound system and is described in US patent 5,997,479 (Savord et al.) and in US patent 6,436,048 (Pesque).

**[0025]** The probe is coupled to the scanner 310 of the ultrasound system. The scanner includes a beamform controller 312 which is responsive to a user control and provides control signals to the microbeamformer 502 instructing the probe as to the timing, frequency, direction and focusing of transmit beams. The beamform controller also control the beamforming of received echo signals by its coupling to the analog-to-digital (A/D) converters 316 and the beamformer 116. Echo signals received by the probe are amplified by preamplifier and TGC (time gain control) circuitry 314 in the scanner, then digitized by the A/D converters 316. The digitized echo signals are then formed into beams by a beamformer 116. The echo signals are then processed by an image processor 318 which performs digital filtering, B mode detection, and/or Doppler processing, and can also perform other signal processing such as harmonic separation, speckle reduction through frequency compounding, and other desired image processing.

**[0026]** The echo signals produced by the scanner 310 are coupled to a display subsystem 320, which processes the echo signals for display in the desired image format. The echo signals are processed by an image line processor 322, which is capable of sampling the echo signals, splicing segments of beams into complete line signals, and averaging line signals for signal-to-noise improvement or flow persistence. The image lines of each biplane image are scan converted into the desired image format by a scan converter 324 which performs R-theta conversion as is known in the art. The images are then stored side-by-side (see FIGURE 10) in an image memory 328 from which they can be displayed as one display frame on the display 150. The images in memory are also overlaid with graphics to be displayed with the images, which are generated by a graphics generator 330 which is responsive to a user control. Individual image frames or image frame sequences can be stored in a cine memory 326 during capture of image loops.

**[0027]** For real-time volumetric imaging the display subsystem 320 also includes the 3D image rendering processor 162 which receives image lines from the image

line processor 322 for the rendering of a real-time three dimensional image which is displayed on the display 150.

**[0028]** In accordance with the principles of the present invention, the biplane system includes an automatic border detection (ABD) processor 470 which operates as described above in real time to automatically trace the myocardial borders of the biplane images as they are produced. The result of border tracing of orthogonal biplane LV images is shown in the user display of FIGURE 12 which is that of a constructed embodiment of the present invention. In the embodiment of FIGURE 12, the display screen is divided into four quadrants. In the upper left quadrant one of the biplane images is shown with the heart walls (endocardium 210 and epicardium 214) delineated by automatically drawn traces produced by the ABD processor and overlaid over the ultrasound image by the graphics generator 330. The orientation of the image plane of the ultrasound image in quadrant 202 is seen to be zero degrees.

**[0029]** A biplane image in a 90° orthogonal plane is shown in the upper right quadrant 204. Like the first biplane image, the epicardium 216 and endocardium 212 of the LV have been delineated by automatically drawn borders.

**[0030]** A graphical model of the LV chamber volume produced as an interpolated surface spline 220 is shown in the lower left quadrant 206 of the display. This surface spline is formed in this embodiment by fitting a surface to the orthogonal borders 210 and 212 as discussed below. The surface spline 220 encloses a volume which is measured by Simpson's formula (rule of disks) to estimate the instantaneous capacity of the LV at each time of biplane image acquisition. These quantitative volume measures are displayed as a function of time in the lower right quadrant 208 as illustrated by the physiologic curve 218 of the LV volume. Numeric measures of the volume at end diastole and end systole are shown to the right of the physiologic curve 218.

**[0031]** While various processes may be used to produce the spline surface 220 in FIGURE 12, the technique used in a constructed embodiment is illustrated by FIGURES 13a and 13b. In the perspective view of FIGURE 13a the two tracings 210 and 212 of the endocardial border of the simultaneous biplane images are shown on a base 220 which represents the mitral valve plane. The apex marker is shown at 230. In this example the image planes of the two biplane images are orthogonal to each other. The volume within the two tracings 210 and 212 is mathematically divided into spaced planes 222 which are parallel to the base plane 220. These planes intersect the left side of tracing 210 as shown at a,a and intersect the right side of tracing 210 as shown at c,c. The planes intersect the near side of tracing 212 as shown at b,b.

**[0032]** An ellipse is mathematically fit to the four intersection points a,b,c,d of each plane 222 as shown in FIGURE 13b. While curves or splines other than ellipses can be used, including arcs and irregular shapes, an ellipse provides the advantage that Simpson's formula has

been clinically validated when practiced with ellipses. FIGURE 13b shows an ellipse 232 intersecting points a, b,c,d of the two tracings 210,212 near the base 220; an ellipse 234 intersecting the two tracings 210,212 toward the center of the LV volume; and an ellipse 236 intersecting the two tracings 210,212 near the top of the LV volume. When ellipses have been fit on each of the spaced planes 222, the disk-like volumes between the ellipses can be quantified by using the geometries of the adjacent ellipses and the distances between them. The total volume of all of the disk-like volumes is computed by summation to produce an instantaneous measure of the LV volume. The measure is used to produce another point on the physiologic curve 218 and, if the ECG waveform indicates that the heart is at end systole or end diastole, the appropriate numerical value is updated in the lower right quadrant 208 of the display.

**[0033]** In the constructed embodiment a surface is fit to the wire frame model of ellipses and tracings. This can be done by interpolating a surface that fits smoothly over the wire frame. The graphical model 220 of the cavity volume is then displayed with a continuous surface.

**[0034]** In operation, the display of the embodiment of FIGURE 12 appears as follows. With the two dimensional array probe positioned to acquire biplane images intersecting in the vicinity of the apex of the LV, real time biplane images are displayed in the upper quadrants of the display. As each biplane image is acquired a corresponding border is traced on each image by the ABD processor 470 and displayed with the image. Each pair of time-concurrent tracings is used to produce an updated graphical volumetric model corresponding to the tracings of the biplane images at that point in time. An updated quantified volumetric measure of the LV is displayed graphically and/or numerically in the lower right quadrant of the display. As the LV borders of the ultrasound images and their tracings in quadrants 202 and 204 move inward and outward in real time, the graphical volumetric model 220 also swells and recedes correspondingly in real time, and the physiologic curve in the lower right quadrant scrolls in time as it is constantly updated.

**[0035]** It will be appreciated that other variations of the embodiments described above will readily occur to one skilled in the art. For instance, a wide variety of automatic or semi-automatic border detection processes may be used, including those described in US patents 6,491,636 (Chenal et al.); 6,346,124 (Geiser et al.); and 6,106,465 (Napolitano et al.) While the biplane images in the example of FIGURE 12 are shown in orthogonal planes, other planar orientations than 90° may be used. This may be done, for instance, after rotating one of the images as described in my aforementioned US patent 6709394. Instead of using the images from two plane orientations, images from three or more intersecting planes can be acquired, traced, and used to display or quantify volumes or volume measures. Acquiring more images for each volume determination will be more time consuming but

can produce a more anatomically accurate model of the cavity and more accurate volume measurements. Volumes can be defined globally or regionally. For instance, subregions on opposite sides of the LV can be defined by hemi-ellipses or splines and their volumes measured. Volumes which change over time can be identified and measured such as those produced by color kinesis. The volume of interest may be scanned using either a 2D matrix array transducer or a mechanically rotating 1D array transducer. A variety of volume measures may be made, such as ejection fraction and cardiac output determinations. The inventive technique can be used to measure other volumetric objects in the body besides the heart, such as a suspected tumor or anatomy of a developing fetus.

### Claims

1. A method for ultrasonically measuring a volumetric object of a body comprising:
  - acquiring ultrasonic images of the volumetric object in two intersecting image planes at the same time with an ultrasound probe (110);
  - using an automated processor (470) to define corresponding object borders (210, 212) in the ultrasonic images; and
  - producing a graphical model (220) of the volumetric object using the defined corresponding object borders (210, 212), and wherein producing the graphical model (220) comprises producing a wire frame model by fitting a series of curves to the defined corresponding object borders.
2. The method of Claim 1, further comprising producing a display comprising real time images from the two intersecting image planes with the defined corresponding object borders (210, 212) visually highlighted in each image, and a quantified measure using the defined corresponding object borders of the images.
3. The method of Claim 2, wherein producing a display comprising a quantified measure further comprises producing a display of changes in the volumetric object as a function of time.
4. The method of Claim 3, wherein the display of changes in the volumetric object as a function of time comprises a graphical display, a numerical display or both a graphical and a numerical display.
5. The method of Claim 1, wherein acquiring ultrasonic images comprises acquiring ultrasonic images of a chamber of the heart, wherein the corresponding object borders (210, 212)

comprise the wall of the chamber of the heart.

6. The method of Claim 1, further comprising producing quantified measures of the graphical model (220) by the rule of disks.
7. The method of Claim 1, wherein the curves comprise ellipses or hemi-ellipses.
8. The method of Claim 1, wherein the automated processor (470) traces the corresponding object borders in the ultrasonic images.
9. The method of Claim 1, wherein producing the graphical model (220) further comprises fitting a surface to the wire frame model.
10. The method of Claim 1, wherein acquiring comprises acquiring ultrasonic images of the volumetric object in more than two intersecting image planes at the same time with the ultrasound probe (110).

### Patentansprüche

1. Verfahren zur Ultraschallmessung eines volumetrischen Objekts eines Körpers, wobei das Verfahren Folgendes umfasst:
  - gleichzeitiges Erfassen von Ultraschallbildern des volumetrischen Objekts in zwei sich schneidenden Bildebenen mit einer Ultraschallsonde (110);
  - Verwenden eines automatisierten Prozessors (470) zum Definieren entsprechender Objektgrenzen (210, 212) in den Ultraschallbildern; und
  - Erzeugen eines graphischen Modells (220) des volumetrischen Objekts mit Hilfe der definierten entsprechenden Objektgrenzen (210, 212), und wobei das Erzeugen des graphischen Modells (220) das Erzeugen eines Drahtgittermodells (engl. wireframe model) durch Anpassen einer Reihe von Kurven an die definierten entsprechende Objektgrenzen umfasst.
2. Verfahren nach Anspruch 1, das weiterhin das Erzeugen einer Anzeige mit Echtzeitbildern anhand der beiden sich schneidenden Bildebenen mit visuell hervorgehobenen definierten entsprechenden Objektgrenzen (210, 212) in jedem Bild, und mit einem quantifizierten Maß unter Verwendung der definierten entsprechenden Objektgrenzen der Bilder umfasst.
3. Verfahren nach Anspruch 2, wobei das Erzeugen einer Anzeige mit einem quantifizierten Maß weiterhin das Erzeugen einer Anzeige von Änderungen in

dem volumetrischen Objekt als eine Funktion der Zeit umfasst.

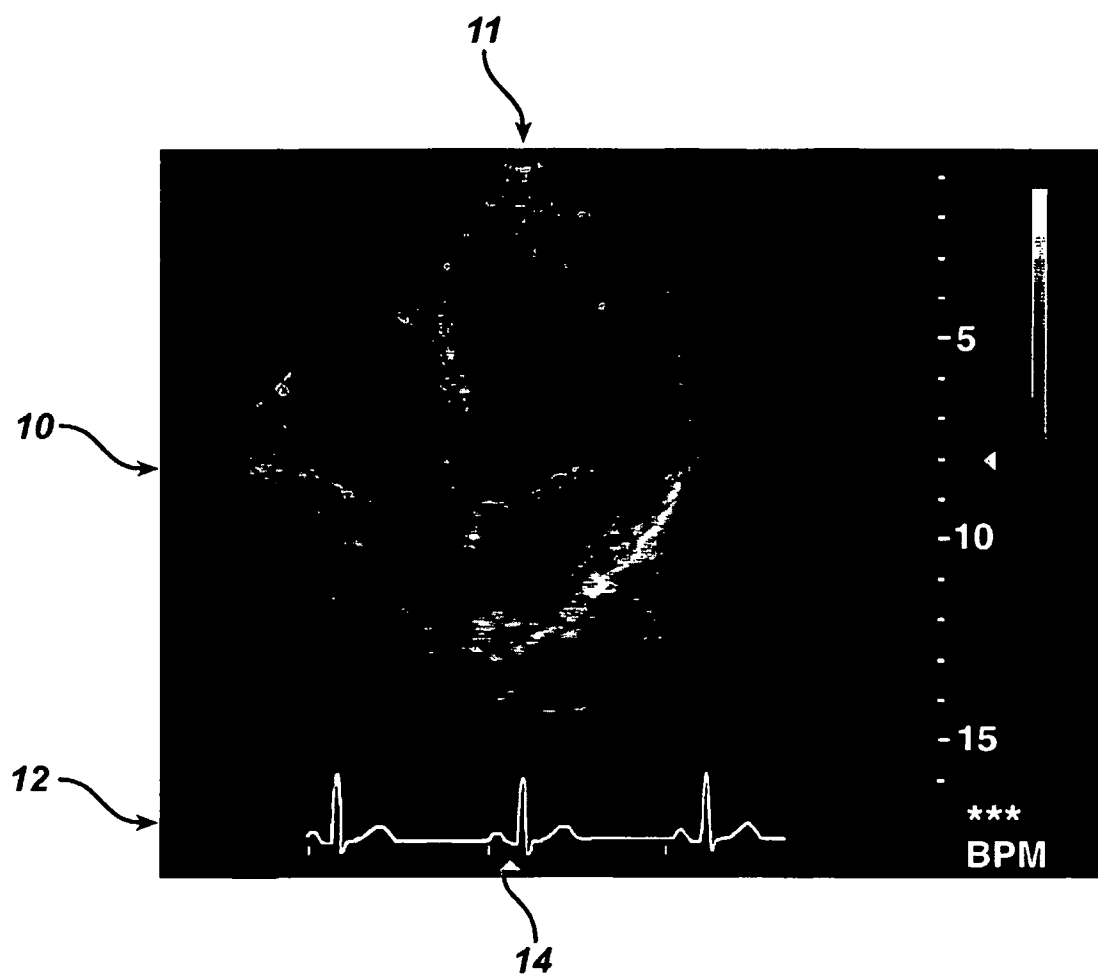
4. Verfahren nach Anspruch 3, wobei die Anzeige von Änderungen in dem volumetrischen Objekt als eine Funktion der Zeit eine graphische Anzeige, eine numerische Anzeige oder sowohl eine graphische als auch eine numerische Anzeige umfasst.
5. Verfahren nach Anspruch 1, wobei das Erfassen von Ultraschallbildern das Erfassen von Ultraschallbildern einer Herzkammer umfasst, wobei die entsprechenden Objektgrenzen (210, 212) die Wand der Herzkammer umfassen.
6. Verfahren nach Anspruch 1, das weiterhin das Erzeugen quantifizierter Maße des graphischen Modells (220) mittels der Scheibenregel umfasst.
7. Verfahren nach Anspruch 1, wobei die Kurven Ellipsen oder Hemi-Ellipsen umfassen.
8. Verfahren nach Anspruch 1, wobei der automatisierte Prozessor (470) die entsprechenden Objektgrenzen in den Ultraschallbildern verfolgt.
9. Verfahren nach Anspruch 1, wobei das Erzeugen des graphischen Modells (220) weiterhin das Anpassen einer Oberfläche an das Drahtgittermodell umfasst.
10. Verfahren nach Anspruch 1, wobei das Erfassen weiterhin das gleichzeitige Erfassen von Ultraschallbildern des volumetrischen Objekts in mehr als zwei sich schneidenden Bildebenen mit der Ultraschallsonde (110) umfasst.

## Revendications

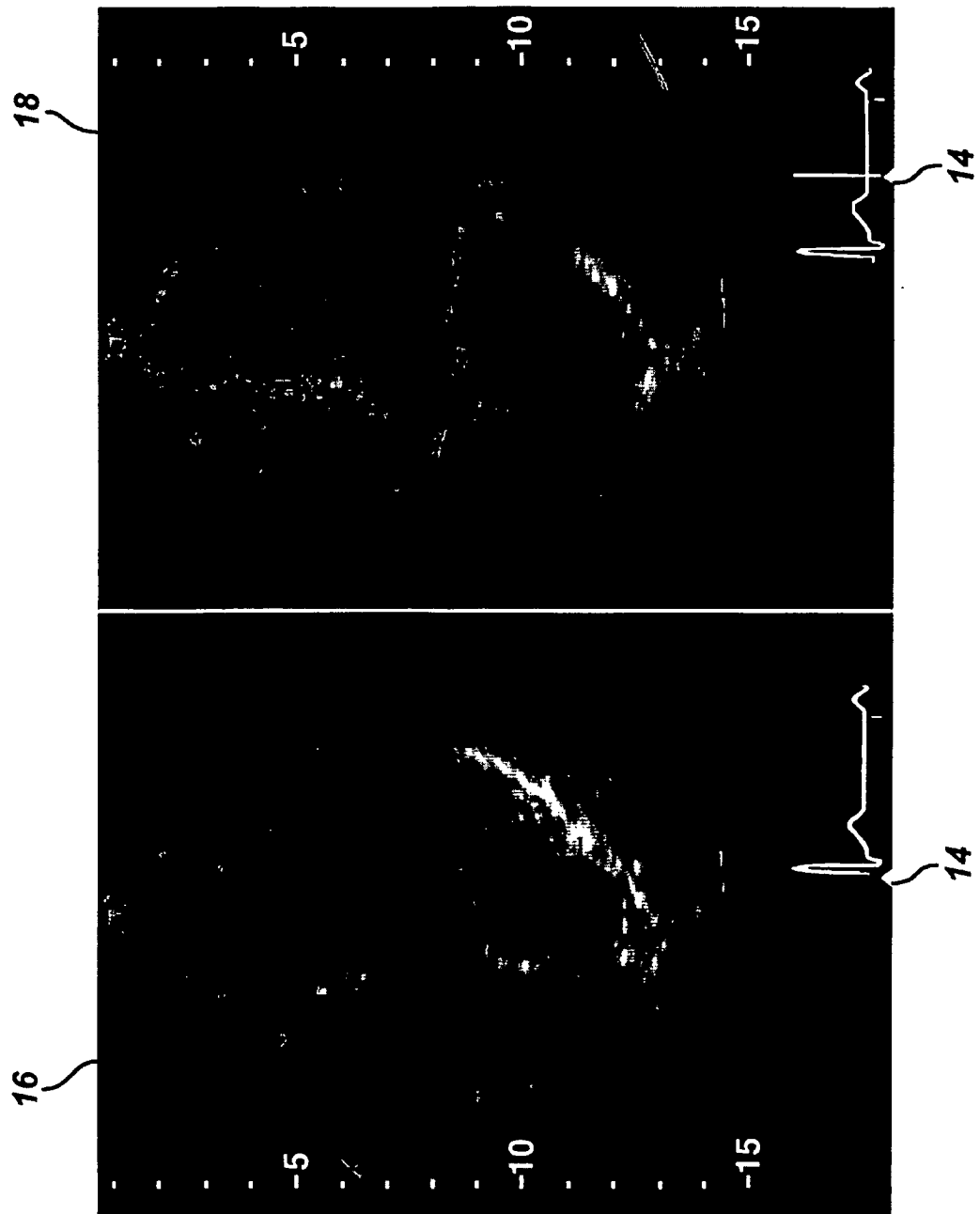
1. Procédé pour mesure de façon ultrasonique un objet volumétrique d'un corps comprenant :  
l'acquisition d'images ultrasoniques de l'objet volumétrique dans deux plans d'image qui se croisent en même temps avec une sonde à ultrasons (110) ;  
l'utilisation d'un processeur automatisé (470) pour définir des bordures d'objet correspondantes (210, 212) dans les images ultrasoniques ; et la production d'un modèle graphique (220) de l'objet volumétrique en utilisant les bordures d'objet correspondantes définies (210, 212), et dans lequel la production du modèle graphique (220) produit un modèle fil de fer en ajustant une série de courbe aux bordures d'objet correspondantes définies.

2. Procédé selon la revendication 1, comprenant en outre la production d'un affichage comprenant des images en temps réel à partir des deux plans d'image qui se croisent avec les bordures d'objet correspondantes définies (210, 212) visuellement mises en évidence dans chaque image, et une mesure quantifiée en utilisant les bordures d'objet correspondantes définies des images.
3. Procédé selon la revendication 2, dans lequel la production d'un affichage comprenant une mesure quantifiée comprend en outre la production d'un affichage de changements dans l'objet volumétrique en fonction du temps.
4. Procédé selon la revendication 3, dans lequel l'affichage des changements dans l'objet volumétrique en fonction du temps comprend un affichage graphique, un affichage numérique ou à la fois un affichage graphique et un affichage numérique.
5. Procédé selon la revendication 1, dans lequel l'acquisition d'images ultrasoniques comprend l'acquisition d'images ultrasoniques d'une chambre du coeur, dans lequel les bordures d'objet correspondantes (210, 212) comprennent la paroi de la chambre du coeur.
6. Procédé selon la revendication 1, comprenant en outre la production de mesures quantifiées du modèle graphique (220) par la règle des disques.
7. Procédé selon la revendication 1, dans lequel les courbes comprennent des ellipses ou des demi-ellipses.
8. Procédé selon la revendication 1, dans lequel le processeur automatisé (470) trace les bordures d'objet correspondantes dans les images ultrasoniques.
9. Procédé selon la revendication 1, dans lequel la production du modèle graphique (220) comprend en outre l'ajustement d'une surface au modèle fil de fer.
10. Procédé selon la revendication 1, dans lequel l'acquisition comprend l'acquisition d'images ultrasoniques de l'objet volumétrique dans plus de deux plans d'image qui se croisent en même temps que la sonde à ultrasons (110).

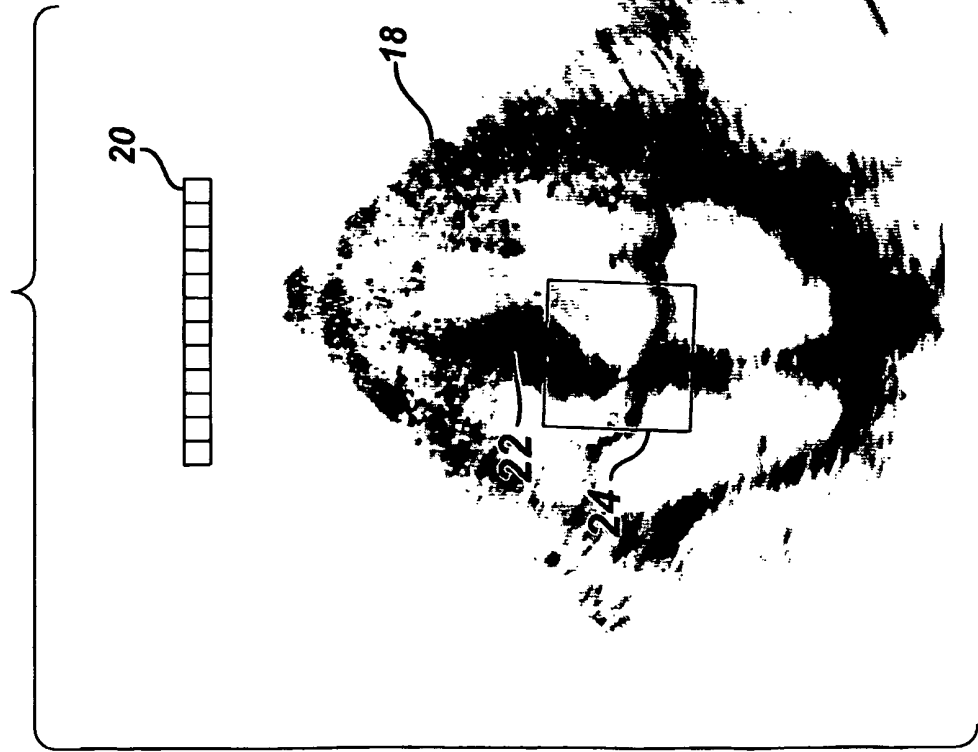
**FIG. 1**



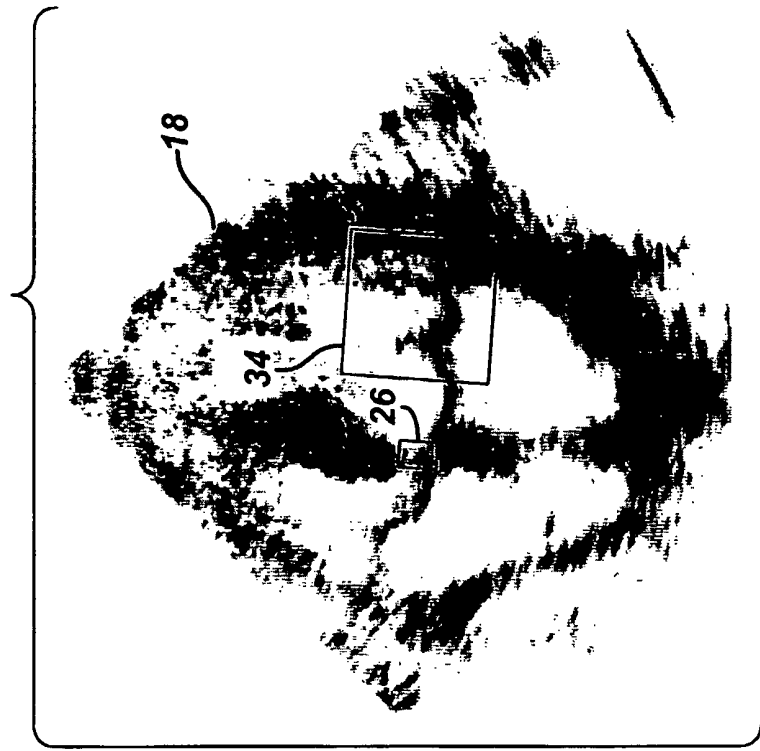
**FIG. 2**



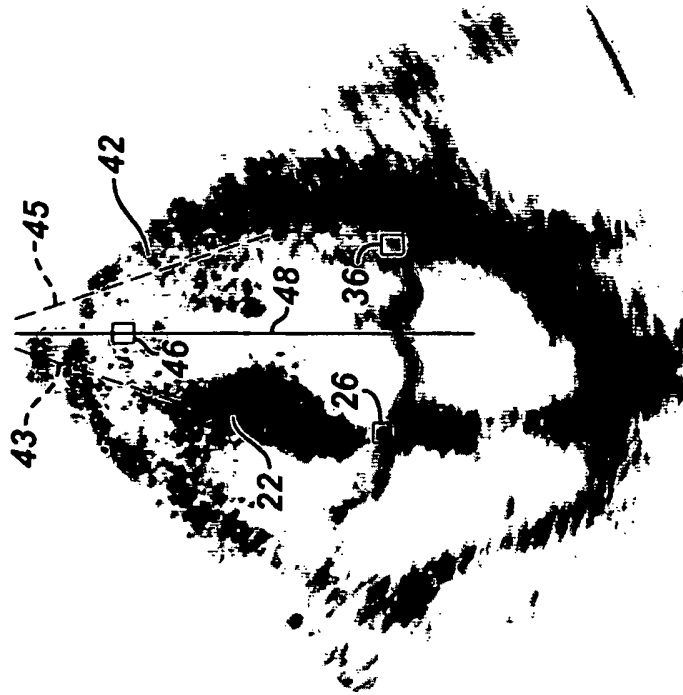
**FIG. 3a**



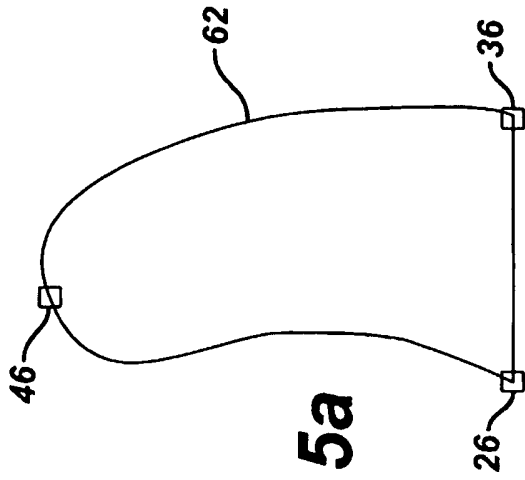
**FIG. 3b**



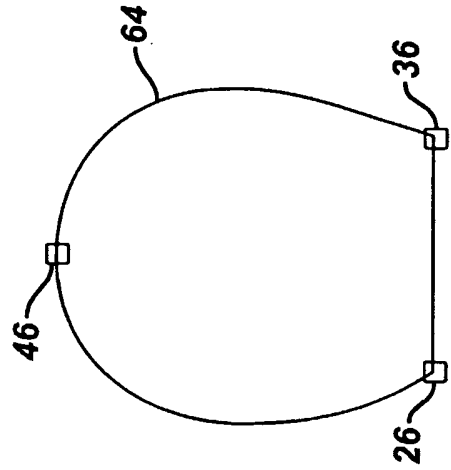
**FIG. 4**



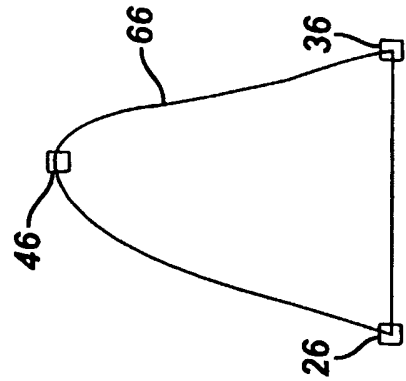
**FIG. 5a**



**FIG. 5b**



**FIG. 5c**



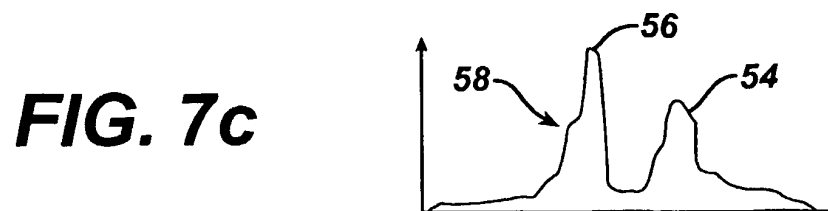
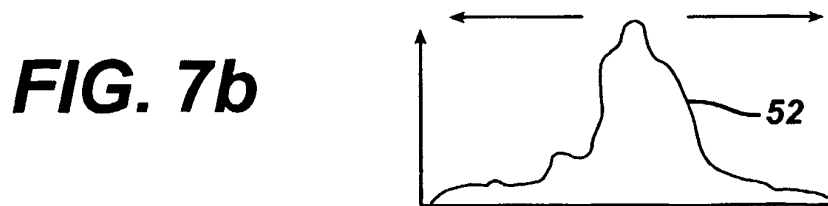
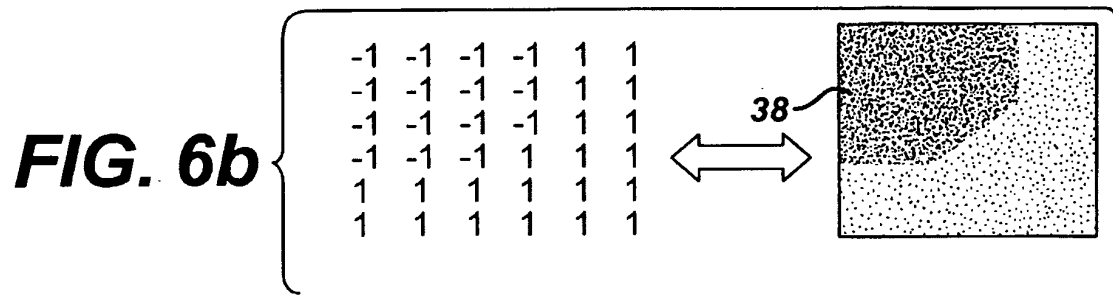
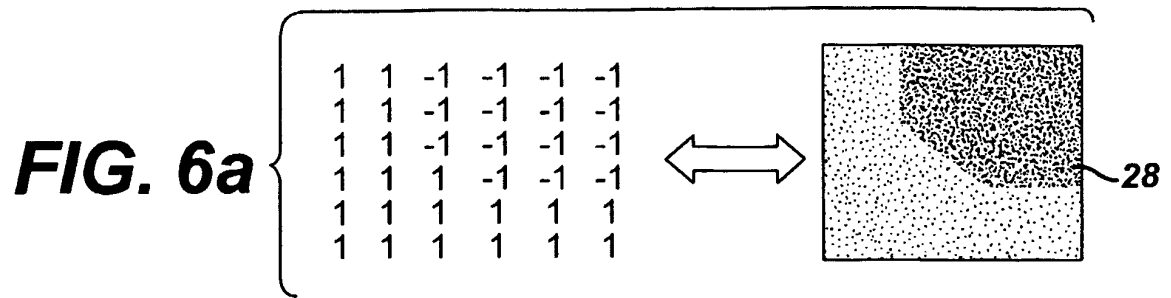
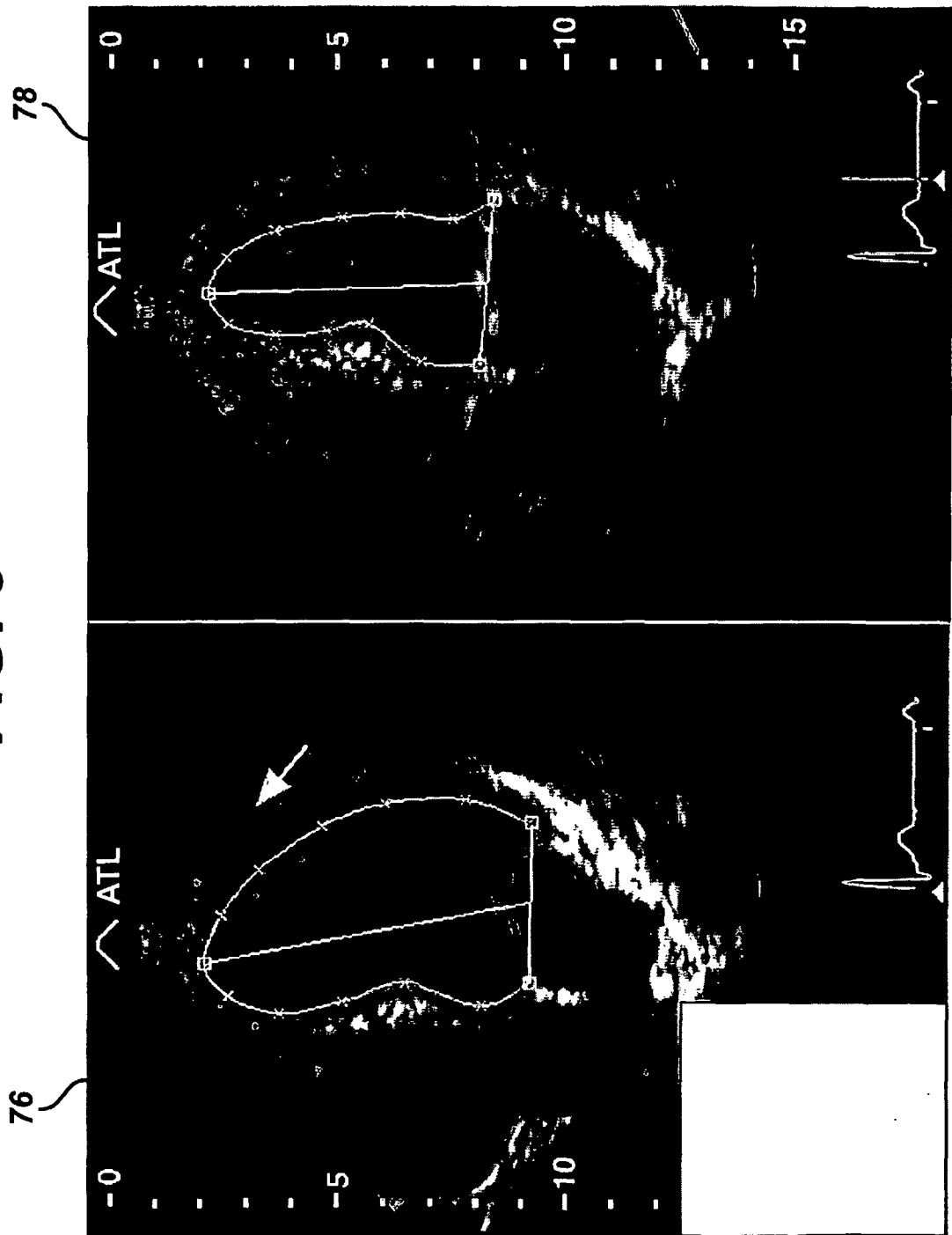
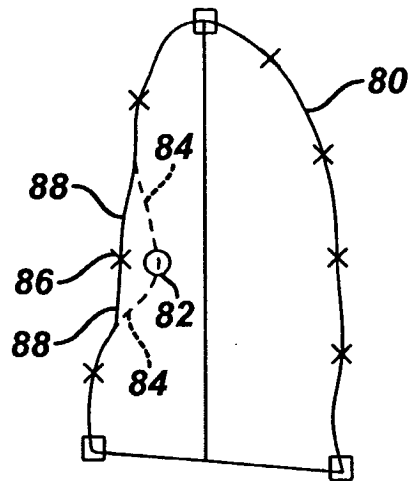


FIG. 8

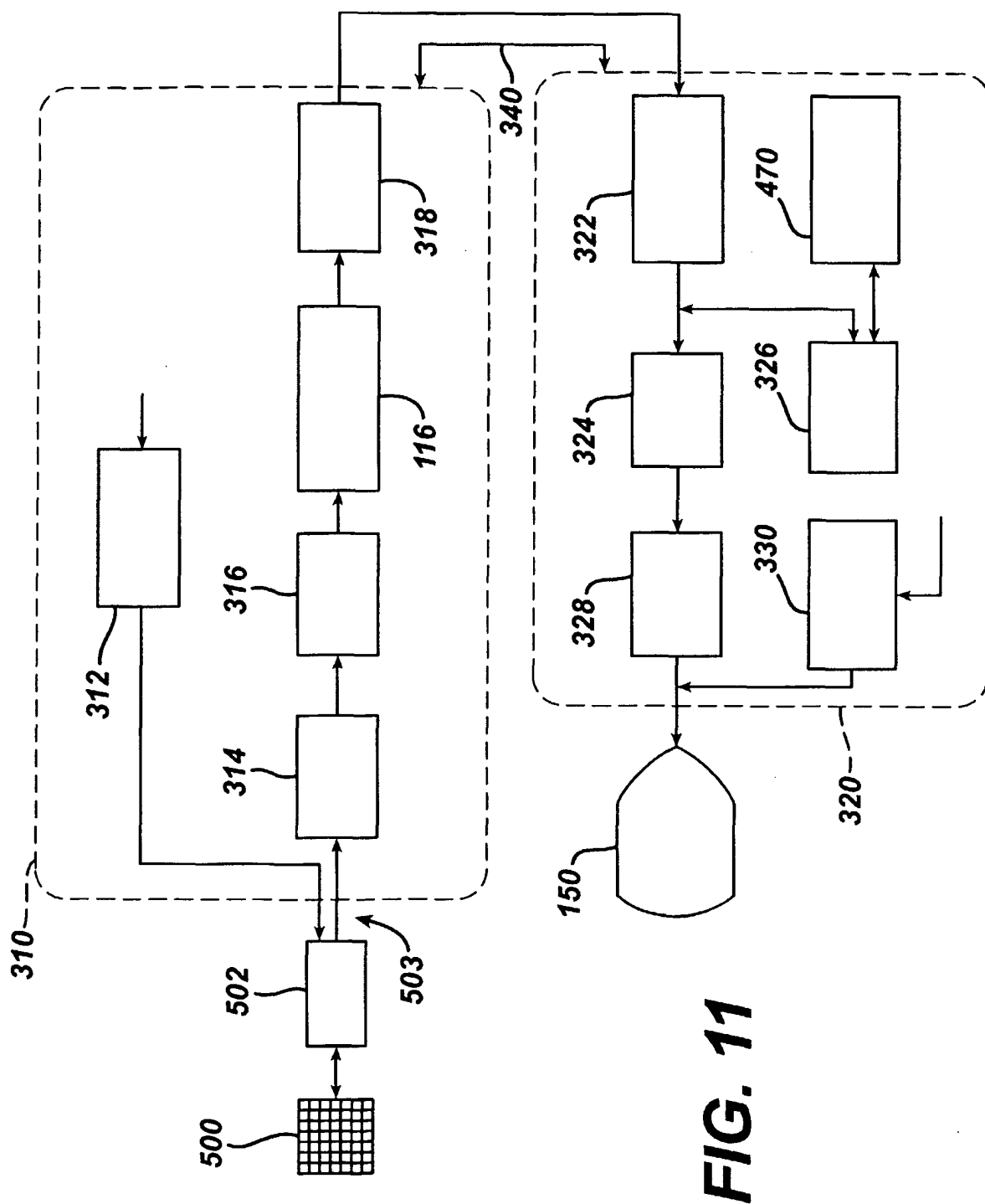


**FIG. 9**



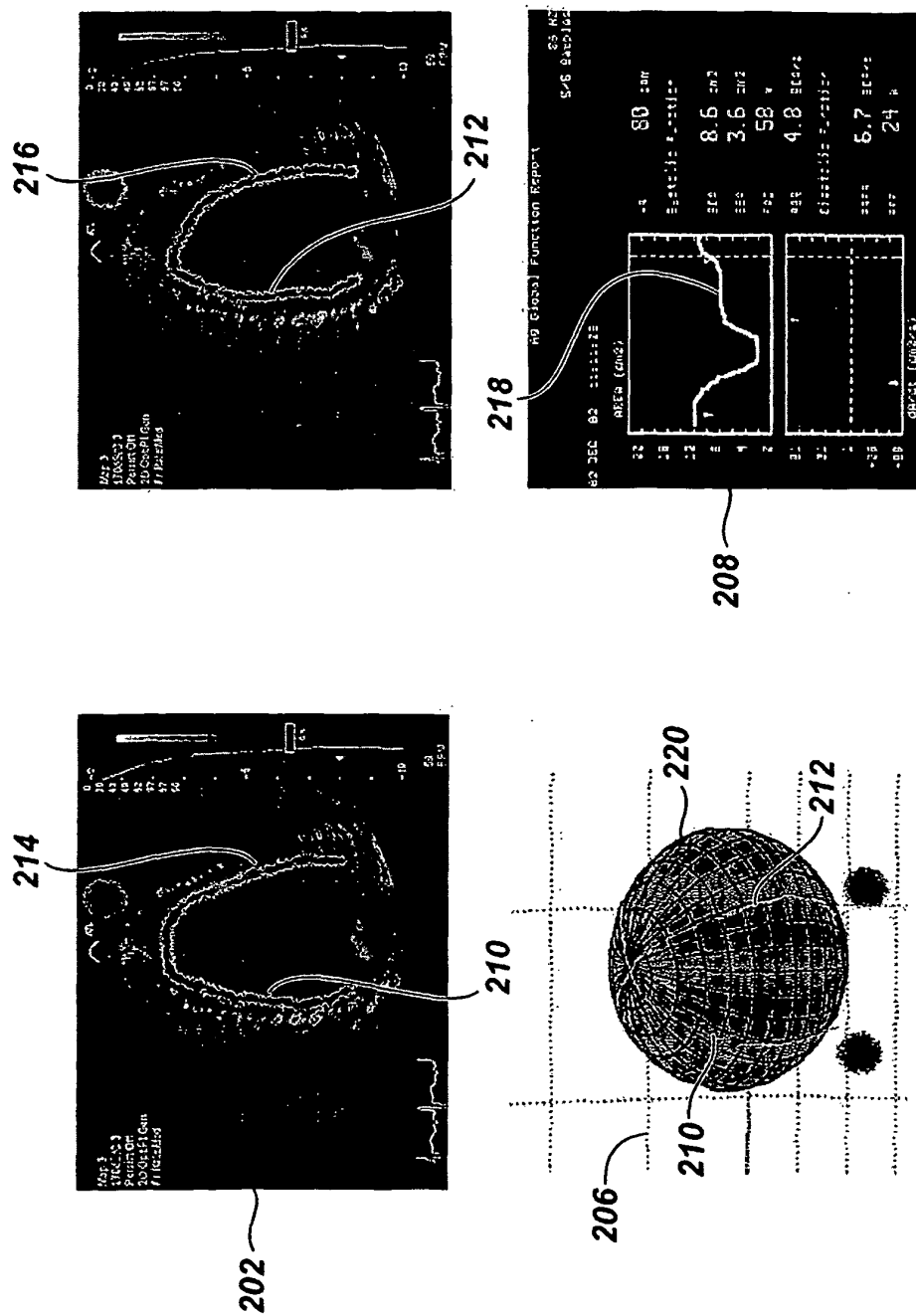
**FIG. 10**

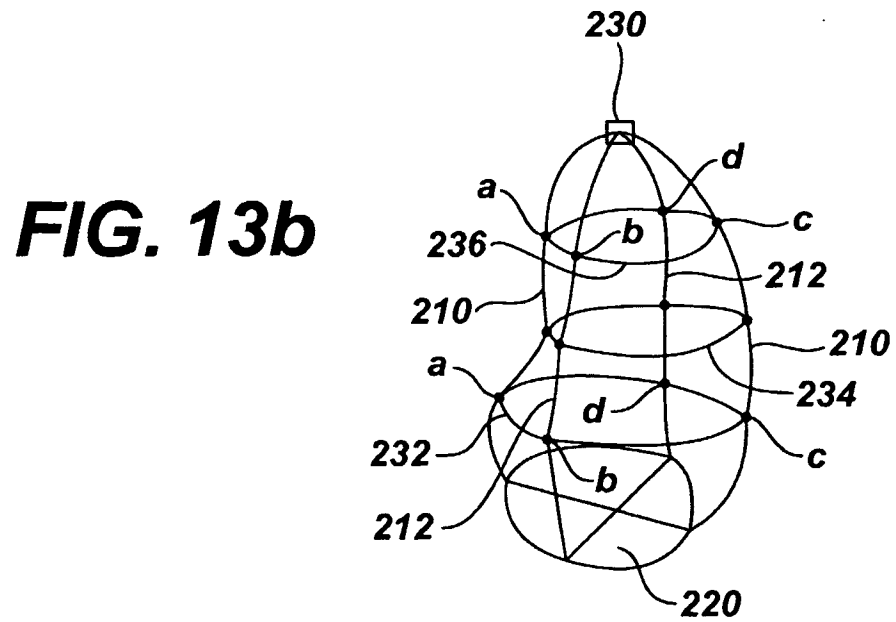
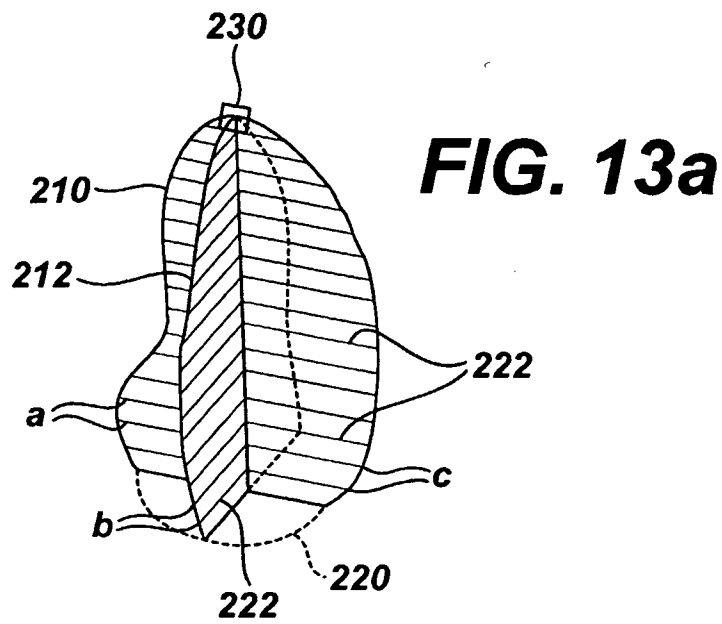




**FIG. 11**

**FIG. 12**





**REFERENCES CITED IN THE DESCRIPTION**

*This list of references cited by the applicant is for the reader's convenience only. It does not form part of the European patent document. Even though great care has been taken in compiling the references, errors or omissions cannot be excluded and the EPO disclaims all liability in this regard.*

**Patent documents cited in the description**

- US 5322067 A, Prater **[0002]**
- US 20020072671 A **[0004]**
- US 6709394 B **[0022]** **[0035]**
- US 5997479 A, Savord **[0024]**
- US 6436048 B, Pesque **[0024]**
- US 6491636 B, Chenal **[0035]**
- US 6346124 B, Geiser **[0035]**
- US 6106465 B, Napolitano **[0035]**

专利名称(译)	超声心脏容量定量		
公开(公告)号	<a href="#">EP1673013B1</a>	公开(公告)日	2010-10-20
申请号	EP2004744758	申请日	2004-08-06
[标]申请(专利权)人(译)	皇家飞利浦电子股份有限公司		
申请(专利权)人(译)	皇家飞利浦电子N.V.		
当前申请(专利权)人(译)	皇家飞利浦电子N.V.		
[标]发明人	SALGO IVAN		
发明人	SALGO, IVAN		
IPC分类号	A61B8/08 G01S15/89 G06F19/00 A61B5/107 G01S7/52 G06T7/60		
CPC分类号	A61B8/0883 A61B5/1075 A61B8/08 A61B8/0858 A61B8/145 A61B8/483 G01S7/52074 G06T7/62 G06T2207/30048		
代理机构(译)	ROCHE , DENIS		
优先权	60/507263 2003-09-29 US		
其他公开文献	EP1673013A1		
外部链接	<a href="#">Espacenet</a>		

#### 摘要(译)

通过获取对象的两个不同图像平面 ( 210,214 ) 的并发双平面图像, 可以超声地进行体内体积对象的量化测量。使用自动边界检测来跟踪体积对象的对应边界。边界描记在其平面空间关系中用于计算体积对象的图形模型 ( 220 )。可以通过盘的规则来计算图形模型 ( 220 ) 的体积, 并且可以显示随时间变化的体积的图形或数字显示。用户界面包括实时双平面图像, 实时图形模型 ( 220 ) 和量化测量。

